NUCL SCI TECH (2020) 31:118
https://doi.org/10.1007/s41365-020-00830-6

Bulk etch rates of CR-39 at high etchant concentrations: diffusion-limited etching

E. M. Awad[1] · M. A. Rana[2] · Mushtaq Abed Al-Jubbori[3]

Received: 18 August 2020 / Revised: 17 October 2020 / Accepted: 19 October 2020 / Published online: 4 December 2020

Abstract Systematic CR-39 bulk etching experiments were conducted over a wide range of concentrations (2–30 N) of NaOH-based etchant. Critical analysis and a deep discussion of the results are presented. A comprehensive nuclear track chemical etching data bank was developed. Three regimes of CR-39 bulk etching were identified. Regime I spans etchant concentrations from 2 to 12 N. Regime II spans concentrations from 12 to 25 N. We call this the dynamic bulk etching regime. Regime III is for concentrations greater than 25 N. In this regime, the bulk etch rate is saturated with respect to the etchant concentration. This classification is discussed and explained. The role of ethanol in NaOH-based etchants is explored and discussed. A parameter called the "reduced bulk etch rate" is defined here, which helps in analyzing the dependence of bulk etching on the amount of ethanol in the etchant. The bulk etch rate shows a natural logarithmic dependence on the density of ethanol in the etchant.

Keywords CR-39 detector · Ethanol · Bulk etch rate · Reduced bulk etch rate · Diffusion-limited etching · Concentration-limited etching

✉ Mushtaq Abed Al-Jubbori
mushtaq_phy8@yahoo.com;
mushtaq_phy@uomosul.edu.iq; mushtaqphy8@gmail.com

[1] Physics Department, Faculty of Science, Menoufia University, Shebin El-Koom, Menoufia 32511, Egypt

[2] MERADD, Instrumentation Control and Computer Complex (ICCC), PARAS Building, 18-KM Multan Road, P.O. Chung, Lahore, Pakistan

[3] Department of Physics, College of Education for Pure Sciences, University of Mosul, Mosul 41001, Iraq

1 Introduction

A latent or ion track is a damage trail, created by an energetic charged particle, in an insulating solid, commonly known as a solid-state nuclear track detector (SSNTD) [1–3]. The diameter of the latent tracks varies from 2 to 10 nm. Details regarding the structure of latent tracks can be found in several studies [4–7]. Latent tracks can be magnified to the micrometer scale, using appropriate chemical etching, to make them measurable using optical microscopy. Etched tracks are called nuclear tracks, and chemical etching is therefore an essential step in nuclear track detection techniques [8–14].

CR-39 is a highly sensitive and commonly used nuclear track detector [15, 16]. Chemical etching of CR-39 in $NaOH/H_2O$ is a complex process, requiring further study and refinement. It becomes more complex when different amounts of ethanol are added to the $NaOH/H_2O$ etching solution [16–19]. Chemical etching and related methodologies for CR-39 detectors have been recently investigated by Rana [20] and Awad et al. [21]. The present study extends these studies, especially the study by Awad et al. [21] and Awad and Rana [22]. To explain the extended bulk etch rate values with etchant concentration, they fitted different formulas or empirical models to the experimental data of bulk etching rates of CR-39 over an extensive range of concentrations of NaOH-based aqueous etching solution without ethanol (soft etching) and with the addition of ethanol (strong or fast etching). They described the merits and demerits of fitted formulas. In the present paper, we further analyze the experimental data collected by Awad and his colleagues (Ref. [21] and unpublished data). We provide deep discussion of soft and strong bulk etching of CR-39 to show the role of ethanol in etching, based on

experimental results, calculations and theoretical arguments, in the form of a qualitative model. The presented model describes the observed features of soft and strong bulk etching, segmenting the extensive range of etching conditions used into three characteristic regimes.

The next section describes the details of the experiments and involved procedures. The results are discussed in Sect. 3, including the above-mentioned qualitative model. Academic and applied conclusions, along with future perspectives, are presented in Sect. 4.

2 Experimental

CR-39 detector plates with thicknesses of 650 μm, manufactured by American Acrylics (US) [20], were cut into pieces, each with an area of 1 cm^2. The prepared CR-39 detector samples were exposed to a ^{252}Cf source one by one for 30 min to achieve optimum fission fragment track statistics ($< 10^4/cm^2$). For exposure, the CR-39 detector was directly placed on a ^{252}Cf source holder. During exposure, the distance between the source and detector was close to 2 mm. Figure 1a is a schematic showing the experimental setup used for the exposure of CR-39 detectors.

The exposed CR-39 detectors were chemically etched to the reveal fission fragment tracks. Fresh NaOH aqueous solution was prepared at concentrations ranging from 2 to 30 N. During the formation of the highest concentration of 30 N, NaOH was fully dissolved and the temperature of the etching solution was increased to 71 °C, which subsequently decreased to 50 °C over 15 min at ambient temperature. Etching solutions was made in glass beakers and the ambient temperature was 19 °C. To each 8 mL of NaOH aqueous solution (2–30 N), various volumes (0, 1, 2 and 3 mL) of ethanol were added to prepare a number of etching solutions for etching of exposed CR-39 detectors. The concentration variations of the prepared etching solutions from the set values were less than 1%. The etching

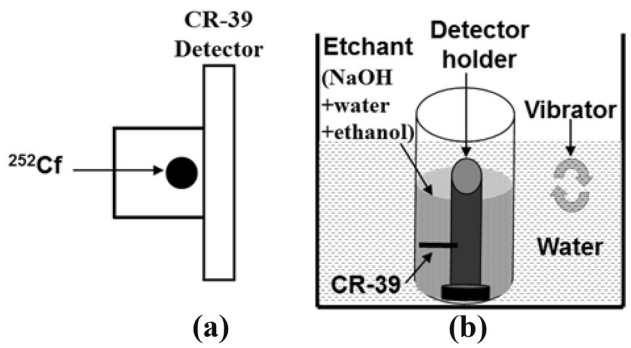

Fig. 1 **a** Fission fragment exposure setup and **b** chemical etching setup for etching of exposed CR-39 detectors

temperature was 70 °C, and its maximum variation was 1 °C. During etching, active shaking was maintained to keep the etching solution uniform and for quick removal of etch products from the growing narrow tracks. The vibrator in Fig. 1b appears gray, as it is shown inside the water bath around the etching beaker. The schematic diagram in Fig. 1b shows the processes involved in a simplistic manner. It should be noted that in the reality, the vibrator or shaking base was holding etching beakers which were 9 in number. The viscosities of the etching solutions were determined using the viscous flow time method [23, 24] at an etching temperature of 70 °C. Figure 1b is a schematic of the experimental setup used for the etching of CR-39 detectors. Etching time was varied for different etching conditions to keep the removed bulk etch layer for each case close to 10 μm. This was done because of the limited range ($\sim$ 15–20 μm) of fission fragments in CR-39 detectors. The etching time for the softest etching condition (8 ml of 2 N NaOH aqueous solution + 0 mL of ethanol) was 16.6 h while it was 2.5 min for the strongest etching condition (8 mL of 30 N NaOH aqueous solution + 3 mL of ethanol). The maximum uncertainty in etching time intervals was estimated to be 20 s. It is worth mentioning that it took approximately 1 min to heat the etching solutions to 70 °C for all investigated etching conditions, as the amounts of the etching solutions were only 8 to 9.0 mL. Because of the standard miscibility of NaOH aqueous solution and ethanol, the total volume of the etching solution was $\approx$ 8 mL when 1 mL of ethanol was mixed with 8 mL of NaOH aqueous solution. The total volume of etching solution was $\approx$ 8.5 mL when 2 mL of ethanol was mixed with 8 mL of NaOH aqueous solution and similarly it was $\approx$ 9.0 mL when 3 ml of ethanol was mixed with 8 ml of NaOH aqueous solution. Readers are encouraged to read an investigation by Yanagie et al. [25] with a very interesting narrative of chemical etching.

After etching of the exposed CR-39 detectors, the diameters of the fission fragment tracks were measured manually using an optical microscope (OPTIKA B-1000BF-ALC, Italy). Care was taken not to include microscopic scratches and cracks in the measured fission fragment tracks. The measurement resolution of track diameters was $\pm$ 0.5 μm. The diameters of 40 circular tracks were measured corresponding to each of the etching conditions used. The mean values of track diameters and related uncertainties or standard deviations were determined from collected physical data using the computer program OriginLab (https://www.originlab.com). The bulk etch rates of CR-39 detectors under various etching conditions were determined using the following well-known formula:

$$V_b \approx \frac{D_{ff}}{2t_e}, \quad (1)$$

where V_b is the bulk etch rate, D_{ff} is the mean diameter of the fission fragment tracks etched under specific etching conditions and t_e is the etching time.

Table 1 shows the fission track diameter data bank, resulting from a set of systematic fission track etching experiments, for measurement of the bulk etch rates of CR-39 detectors under various etching conditions ($NaOH/H_2O$ + ethanol at 70 °C). Different etching time intervals were used to obtain total bulk etching up to ~ 10 µm. A limit of 10 µm was observed considering the limited etchable range of fission fragments in the CR-39 polymer. Uncertainties or standard deviations of the track diameters are also presented. The essential information, related to the data bank (Table 1), is clearly described. A single tabulation of the data, along with analysis plots in the next section, is provided for easy access of the data to users of nuclear track etching over a broad range of chemical etching conditions. Table 1 is a comprehensive nuclear track chemical etching data bank that was developed in a unique manner. The developed data bank has a number of uses in nuclear track research and applications. It can be used to design new chemical etching experiments in the studied zones of etching conditions.

3 Results and discussion

The bulk etch rates, V_b, at the shallow surface layers of the CR-39 detector with a depth of ~ 10–15 µm were calculated using Eq. (1). This equation assumes the linear dependence of fission track diameters with etching time, $D_{ff}(t_e)$, which has been proven as shown in Fig. 2a. In this figure, the diameter growth of fission fragment tracks with etching time in the soft regime (Regime I) where no ethanol was added was investigated taking into account the 0 point. For soft etching the linear dependence of D_{ff} on the etching time is expected. However, the current study examines this assumption for higher growth bulk etch rates. The diameter growth of fission fragment tracks with etching time in the soft and active regimes (Regime I and Regime II) where 3 mL ethanol was added (highest etching rates in this study) show that the linear dependence of $D_{ff}(t_e)$, still applicable despite the fact that growth is high and with large steep growth, as shown in Fig. 2b.

The bulk etch rates of CR-39 were studied over an extensive range of etching concentrations, Fig. 3a. The etching solutions were prepared by mixing NaOH, water and ethanol in various proportions. This plot (Fig. 3a) provides detailed deep information about the bulk etching behavior with varying etchant concentration. Bulk etching is the inverse process of aggregation or deposition at the atomic or molecular scale. Before discussing of the plot in Fig. 3a, it is worth noting that important steps in chemical bulk etching are penetration of the etchant into the polymer bulk, reaction of the etchant with weaker bonds in the polymer structure and diffusion of etch products out of the polymer bulk into the etchant. The plot in Fig. 3a can be characterized into three regimes resulting from the complex roles of the concentration of the $NaOH/H_2O$ etching solution and the amount of ethanol added to the etching solution. The dependence of the bulk etch rate on the NaOH concentration in Fig. 3a is more systematic for the case of no ethanol than for the cases of added ethanol. The addition of different amounts of ethanol in the $NaOH/H_2O$ etching solution significantly enhanced the values of the bulk etch rate regardless of the jumps in the V_b values. Clearly, harsh etching produces slightly irregular results as expected.

The growth of the bulk etch rate with etchant concentration was not systematic and requires careful inspection. Therefore, it has been divided into three regimes. Regime I spans etchant concentrations from 2 to 12 N. This is a concentration-limited regime. In this regime, the concentrations of the etchant are too small for the bulk etching process. The bulk etch rate increases weakly with concentration in this regime, producing systematic results for the addition of 1 and 2 mL of ethanol and for 3 mL ethanol up to 8 N NaOH. In this regime, a slow reaction rate is dominant and the Arrhenius equation is applicable. Regime II is very important from an operational perspective. It spans concentrations from 12 to 25 N. We call this the dynamic bulk etching regime. In this regime, the bulk etch rate grows actively with etchant concentration in some sense from proportional to exponential. Etching in the dynamic regime can be used to fabricate track etched membranes from thick CR-39 plates, irradiated with swift heavy ions and many other applications where fast etching (or short etching time) is required [26]. Regime III denotes concentrations greater than 25 N. In this regime, the bulk etch rate saturated with respect to the etchant concentration. Limited diffusion of etching species in extremely dense etchant results in the saturation of the bulk etching of CR-39. We call this regime the diffusion-limited regime. The above narrative is called the concentration-diffusion model of bulk etching. Saturation in regime III can be explained in terms of the insulation of etching fronts resulting from deposition of etch products in a highly viscous regime. Stirring in the etching solution during etching, up to a certain limit, can reduce the insulation of etching fronts caused by the deposition of etch products. Active, uniform and quantified stirring of the etching solution should be maintained during precise future etching experiments.

Table 1 Etching time, t_e (min), and corresponding fission track diameters, D (μm), along with standard deviations, σ (μm), for various NaOH concentrations (N) and ethanol volumes (mL). The mean value of dE/dx for fission fragments of ^{252}Cf in CR-39 (at the entrance) is 6578 ± 187 keV/μm

Ethanol volume	0 mL		1 mL		2 mL		3 mL	
NaOH Concentration	t_e (min)	$D\pm\sigma$ (μm)	t_e (min)	$D\pm\sigma$ (μm)	t_e (min)	$D\pm\sigma$ (μm)	t_e (min)	$D\pm\sigma$ (μm)
2 N	573	10.3 + 0.8	368	10.0 + 0.8	330	14.9 + 1.0	125	11.5 + 1.2
	696	13.5 + 1.2	433	12.8 + 1.1	390	17.4 + 1.5	155	12.6 + 0.6
	756	16.0 + 1.2	493	15.1 + 1.5	420	17.6 + 1.2	190	13.8 + 1.3
	816	17.4 + 1.5	553	18.0 + 1.3	460	20.9 + 1.4	220	17.1 + 1.4
	879	20.3 + 1.6	675	22.1 + 1.2				
	1000	22.4 + 1.9						
6.25 N	120	8.6 + 1.2	90	12.6 + 1.5	50	11.5 + 1.5	45	13.8 + 1.2
	140	9.9 + 1.5	100	14.1 + 1.4	60	12.5 + 0.8	50	17.9 + 1.2
	160	12.9 + 1.2	110	16.1 + 1.2	70	15 + 1.1	55	19.8 + 1.4
	180	14.5 + 2.2	120	17.0 + 1.5	80	23.5 + 1.2	60	24.0 + 1.5
			130	18.1 + 1.5				
10 N	30	8.6 + 1.2	30	11.6 + 1.2	20	8.7 + 1.3	10	12.7 + 1.1
	40	11.1 + 1.2	35	13.1 + 1.6	25	14.0 + 1.2	15	21.7 + 1.2
	50	14.5 + 1.5	40	15.1 + 1.7	30	18.5 + 1.2	20	25.5 + 1.9
	60	18.4 + 1.8	45	16.6 + 1.2	35	22.7 + 1.7	25	30.5 + 1.0
			50	19.0 + 1.2	40	25.8 + 1.8		
12 N	40	10.3 + 1.3	30	10.0 + 1.1	20	15.9 + 1.4	10	15.9 + 2.0
	50	12.8 + 1.3	40	14.4 + 1.1	25	19.0 + 1.2	13	20.8 + 1.2
	60	16.0 + 1.2	50	18.1 + 1.6	30	20.4 + 1.4	15	22.9 + 0.9
	70	18.33 + 1.18	60	26.0 + 2.1	35	23.4 + 1.6	17	26.0 + 1.5
					40	26.4 + 1.7		
18 N	25	11.3 + 1.3	10	18.3 + 1.4	6	8.3 + 1.5	3	9.8 + 1.4
	35	17.0 + 1.3	12	21.3 + 1.3	7	13.0 + 1.2	4	16.1 + 1.2
	40	20.3 + 1.1	13	21.9 + 1.6	8	15.5 + 1.3	5	20.4 + 1.6
	45	23.4 + 1.4	14	23.4 + 1.4	10	18.1 + 1.3	6	23.8 + 2.4
					11	20.1 + 1.2		
20 N	20	10.3 + 1.6	5	12.6 + 1.5	4	13 + 1	3	10.6 + 1.9
	30	15.1 + 1.2	6	17.5 + 1.6	5	18.4 + 1.4	4	14.9 + 2.0
	35	18.4 + 1.2	7	20.1 + 1.0	6	23.3 + 1.4	5	19.9 + 1.7
	40	21.3 + 1.5	8	22.3 + 1.4	7	27.3 + 1.6	6	25.4 + 1.2
			9	25.0 + 2.1				
22 N	15	10.4 + 0.9	7	13.3 + 1.1	3	10.9 + 1.1	3	9.0 + 1.2
	20	14.5 + 1.0	8	19.0 + 1.2	4	14.1 + 1.2	4	14.3 + 1.2
	25	18.9 + 1.5	9	20.5 + 1.0	5	19.4 + 1.9	5	19.6 + 1.4
	30	22.1 + 1.2	10	26.4 + 1.5	6	23.9 + 1.5	6	24.0 + 2.4
	35	26.1 + 1.9						
25 N	15	14.5 + 1.9	4	14.6 + 1.4	2	11.3 + 1.3	1.5	10.4 + 0.9
	17	16.6 + 1.4	5	19.9 + 1.5	2.5	19.0 + 1.2	2	15.6 + 1.1
	19	19.0 + 1.2	6	24.1 + 2.1	3	21.4 + 1.5	2.5	19.4 + 1.1
	21	21.0 + 1.2	7	25.8 + 1.4	3.5	26.0 + 1.7	3	22.0 + 1.3
27 N	10	11.6 + 1.2	3	10.3 + 1.1	1.5	9.4 + 1.1	1.5	10.4 + 0.9
	14	16.1 + 1.2	4	14.3 + 1.2	2	13 + 1	2	15.0 + 1.4
	16	18.5 + 1.2	5	16.8 + 1.2	2.5	16.6 + 1.2	2.5	18.1 + 1.1
	18	21.3 + 1.3	6	19.6 + 1.6	3	20.3 + 1.1	3	21.0 + 1.2

Table 1 continued

Ethanol volume	0 mL		1 mL		2 mL		3 mL	
NaOH Concentration	t_e (min)	$D\pm\sigma$ (μm)	t_e (min)	$D\pm\sigma$ (μm)	t_e (min)	$D\pm\sigma$ (μm)	t_e (min)	$D\pm\sigma$ (μm)
	20	23.3 + 1.1	7	23.3 + 1.4	3.5	23.8 + 1.5		
	26	30.8 + 1.1						
30 N	7	9.6 + 0.9	5	14.0 + 1.2	1.5	11.4 + 1.5	1.5	10.5 + 1
	9	12.4 + 1.0	6	18.3 + 1.1	2	15.6 + 1.1	2	14.6 + 1.2
	11	14.9 + 1.1	7	22.5 + 1.8	2.5	19.2 + 1.9	2.5	18.8 + 1.7
	13	18.3 + 1.4	8	25.4 + 2.0				
	15	20.9 + 1.2						
	17	23.1 + 1.1						

The present work focuses on the separation of strong etching from soft etching. Therefore, $V_b(x) - V_b(0)$ was plotted against NaOH/H_2O concentrations for various amounts of added ethanol. $V_b(x)$ is the bulk etch rate with ethanol (x = 1, 2, and 3 mL) and $V_b(0)$ is the bulk etch rate without ethanol in NaOH/H_2O etching solution. $V_b(x)$ is significantly higher than $V_b(0)$ and the term $V_b(x) - V_b(0)$ has a pattern similar to $V_b(x)$, as shown in Fig. 3b. The dependence of viscosity on NaOH concentrations, for various volumes of ethanol used (Fig. 3c), is similar to the dependence of the bulk etch rate on the NaOH concentrations for the same amounts of ethanol (Fig. 3a). The similarity between the trends of bulk etch rate and viscosity growth in the first two regimes is interesting. The viscosity (in Fig. 3c) of the etching solutions could not be measured in Regime III because of the large increase in etchant viscosity in this region and the limitations of the method used.

In addition, a new parameter is introduced to determine the ethanol effect in the etchant solution called the reduced bulk etch rate. It is defined as the ratio of the bulk etch rate with ethanol to the bulk etch rate without ethanol in the NaOH/H_2O etching solutions. Reduced bulk etch rates are plotted against NaOH concentrations in Fig. 4. This parameter elaborates the dependence of the bulk etch rate on the presence of ethanol in the NaOH/H_2O etching solution. In contrast with Fig. 3a, the plot in Fig. 4 is naturally divided into two regimes. Regime I spans NaOH concentrations from 2 to 20 N. Regime II denotes a NaOH concentration greater than 20 N. The reduced bulk etch rate increases with increasing NaOH concentration in Regime I and reaches the maximum value near the boundary between the two regimes. It decreases with increasing NaOH concentration in Regime II. At concentrations greater than 20 N, the effect of ethanol becomes less noticeable. Two major regimes have been distinguished using the suggested reduced bulk etch rate parameters for the ethanol effect. Observation of individual plots in Fig. 3a and Fig. 4, and their comparison demonstrates the complexity of the etching process. The systematics of the plots in Fig. 3a and Fig. 4 are quite different. The role of ethanol is clearer in Fig. 4 than in Fig. 3a. One can see that some jumps in a portion of the data are present in Figs. 3 and 4. This can be explained in terms of the different scales in the two figures and the strong etching process in these regions. Therefore, they are natural because of the harsh or rigorous attack of the etchant on the etching front of the detector at high concentrations of NaOH and ethanol. These etching regions have never been studied before. Ethanol evaporation during the etching process may partly increase the jump in the data. During the etching process, the etchant beaker was covered with a tight lid to reduce ethanol evaporation as much as possible. Systematic data for low NaOH concentrations with added ethanol are obvious. Jumps in the data were more clearly visible with the addition of 3 mL ethanol than with the addition of 2 mL. In general, 1 mL ethanol data (with longer etching times) appeared systematic up to NaOH concentrations of 20 N. Finally, it can be concluded that jumps in the etching data are not due to the evaporation of ethanol, but instead may be a natural consequence of the harsh and strong molecular attack of the etchant solution on the polymer matrix.

Figure 5 shows the analysis of the bulk etches rates of CR-39 with an angle different from that presented in Figs. 3 and 4. Figure 5 is a plot of $\ln(V_b)$ as a function of the ethanol volumes added to the NaOH/H_2O etching solutions. It shows a systematic natural logarithmic dependence of V_b on the ethanol volumes present in NaOH/H_2O etching solutions during etching. It may be noted that the volume of ethanol added to the etching solution is proportional to its concentration in the etching solution.

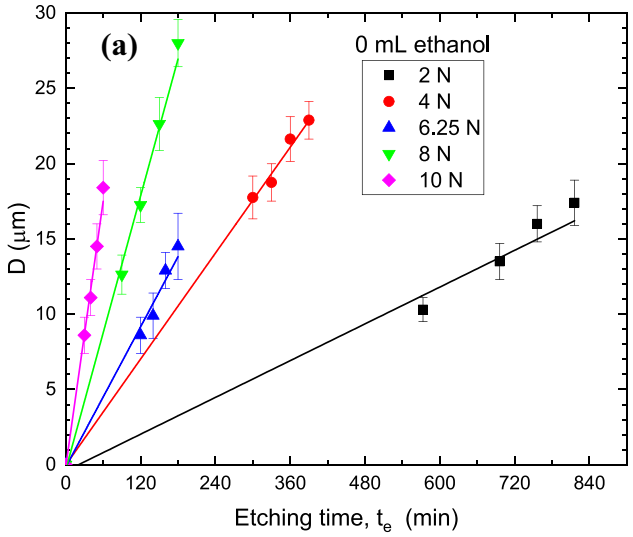

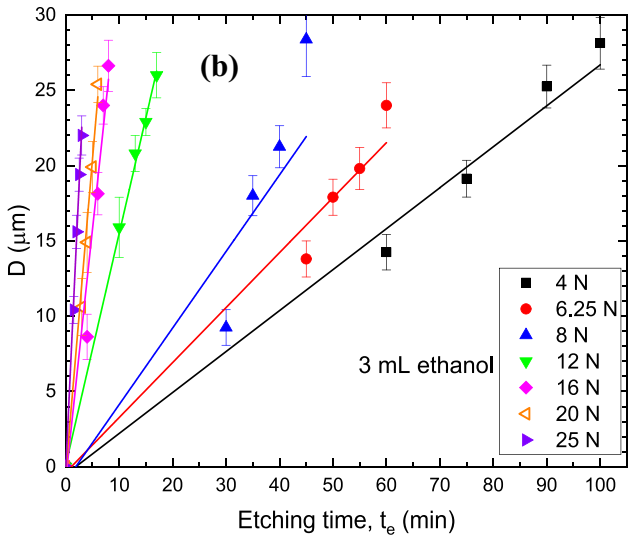

Fig. 2 (Color online) **a** Linear growth of fission fragment tracks diameters with etching time in the soft regime (Regime I) where no ethanol was added. **b** Diameter growth of fission fragment tracks with etching time in the soft and active regimes (Regime I and Regime II) where ethanol was added showing that the linear dependence of D (t) is still applicable

A careful examination of the visual appearance of fission tracks and the background in CR-39 detectors, etched under various etching conditions, was carried out using optical microscopy. Extreme etching conditions should be avoided unless they are required. Extreme etching conditions refer to the lowest and the highest concentrations of etching solutions. Selected optical micrographs of CR-39 detectors, showing etched tracks and background surface, are presented in Fig. 5. One can observe track scratches and some irregularity in fission tracks at higher concentrations of NaOH and ethanol as a result of the rigorous attack of the etching solution. The reason for the slight lack of clarity of the fission tracks in Fig. 6 is due to the

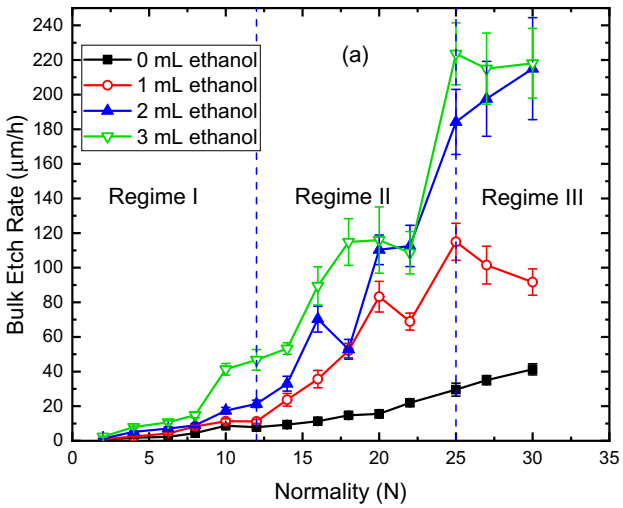

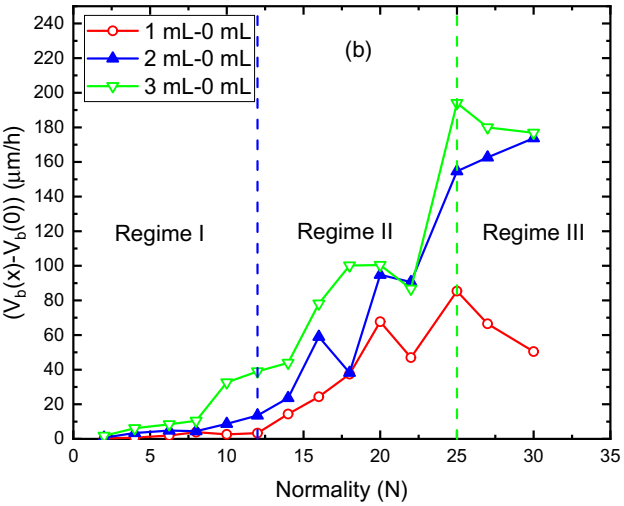

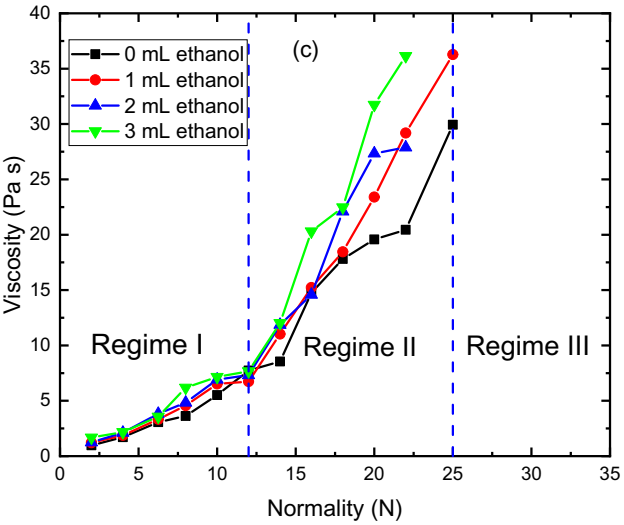

◀**Fig. 3** (Color online) **a** Bulk etch rate of CR-39 as a function NaOH/H_2O concentration with various amounts of added ethanol. Error bars in the plot show the amounts of error in the plotted values of bulk etch rate. **b** $V_b(x)$-$V_b(0)$ as a function of NaOH/H_2O concentration. $V_b(x)$ is the bulk etch rate of CR-39 for "x" volume of ethanol, added to the etching solution NaOH/H_2O. The variable "x" refers to 1, 2 or 3 mL of ethanol. $V_b(0)$ is the bulk etch rate of CR-39 in NaOH/H_2O without ethanol. **c** Measured viscosity of the NaOH/H_2O etching solution for various amounts of added ethanol. Fluctuations are not deterministic but are of random nature. Fluctuations are due to the uncertainty introduced by the limited diffusion of both etching solution and etch products during etching. However, this study requires further investigation from other independent researchers for further confirmation

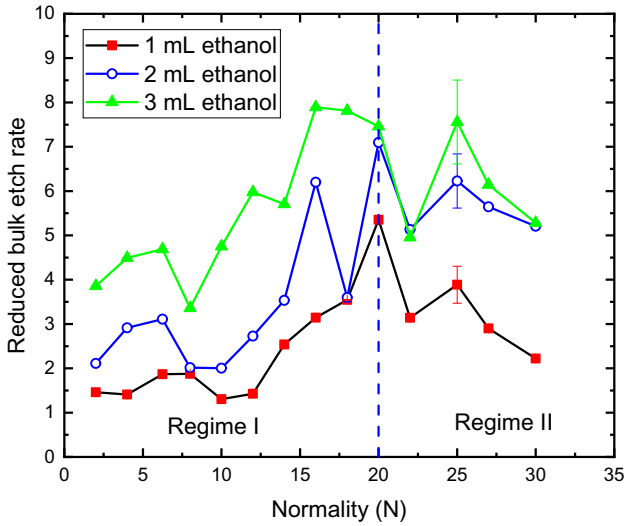

Fig. 4 (Color online) Reduced bulk etch rate as a function of NaOH/H_2O concentration for various amounts of added ethanol. Errors in the reduced bulk etch rate are shown only for 25 NaOH/H_2O cases to avoid complexity in the plot

overlapping of a comparatively large of number of accompanied alpha tracks that were at the stage of initial growth. The micro-scale appearance of alpha tracks starts at considerably higher etching times.

Based on our careful optical examination and measurements, a schematic presentation showing NaOH concentrations on the x-axis and ethanol density on the y-axis is illustrated in Fig. 7. The area of the schematic plot in Fig. 7 can be divided into five zones. These zones include the "soft etching zone", "harsh etching zone", two "semi-harsh etching" zones and the central "optimum etching zone". The characteristics of the "semi-harsh" zone along the NaOH concentration axis are different from the "semi-harsh" zone along the ethanol concentration axis. Our results are qualitatively in line with recent investigations [27, 28] which have employed similar etching solutions containing KOH, water and ethanol.

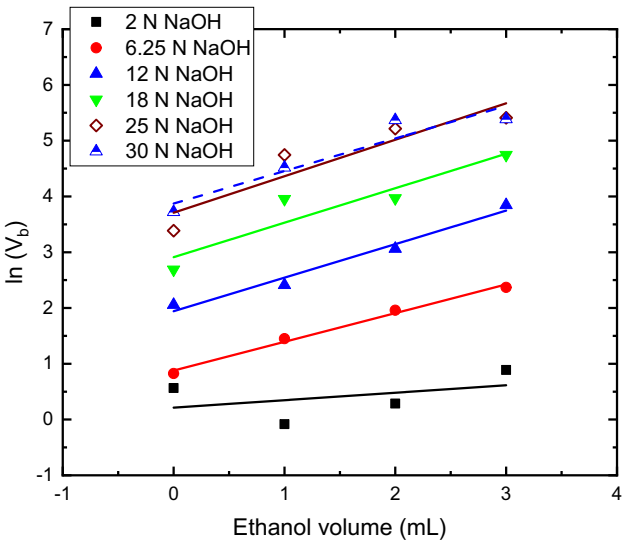

Fig. 5 (Color online) Plot of ln(V_b) as a function of amount of ethanol added to NaOH/H_2O etching solution for various values of NaOH concentrations

4 Conclusions and future perspective

Chemical etching of bulk and nuclear tracks is a complex process because of the nature of the polymer bond strengths, manufacturing process and lack of precise control over etching species during etching. Variations in the material and chemical structure of different versions or lots of the same track detector contribute greatly to the complexity of the chemical etching behavior. Variations in the concentration of etching species and temperature profile of the etching solution can also be sources of complexity. Adding ethanol to a NaOH/H_2O solution of CR-39 detectors is a simple way to accelerate the chemical etching process and to shorten the etching time. It can be used in many applications. The addition of ethanol to the NaOH/H_2O etching solution of CR-39 detectors increases the reaction rate further and hence adds more complexity to the process of chemical etching. However, the linear growth of fission fragment track diameters with etching time is still applicable for etching without ethanol (soft) and with ethanol (soft and active).

Three regimes of CR-39 bulk etching were identified as follows: Regime I spans etchant concentrations from 2 to 12 N. This is a concentration-limited regime. In this regime, the concentrations of the etchant are too small for the bulk etching process and the reaction rate follows the Arrhenius equation (soft etching zone). The bulk etch rate increases weakly with concentration in this regime. Regime II is very important from an operational perspective. It spans concentrations from 12 to 25 N. We call this the dynamic bulk etching regime. In this regime, the bulk etch rate grows actively with the etchant concentration, in some

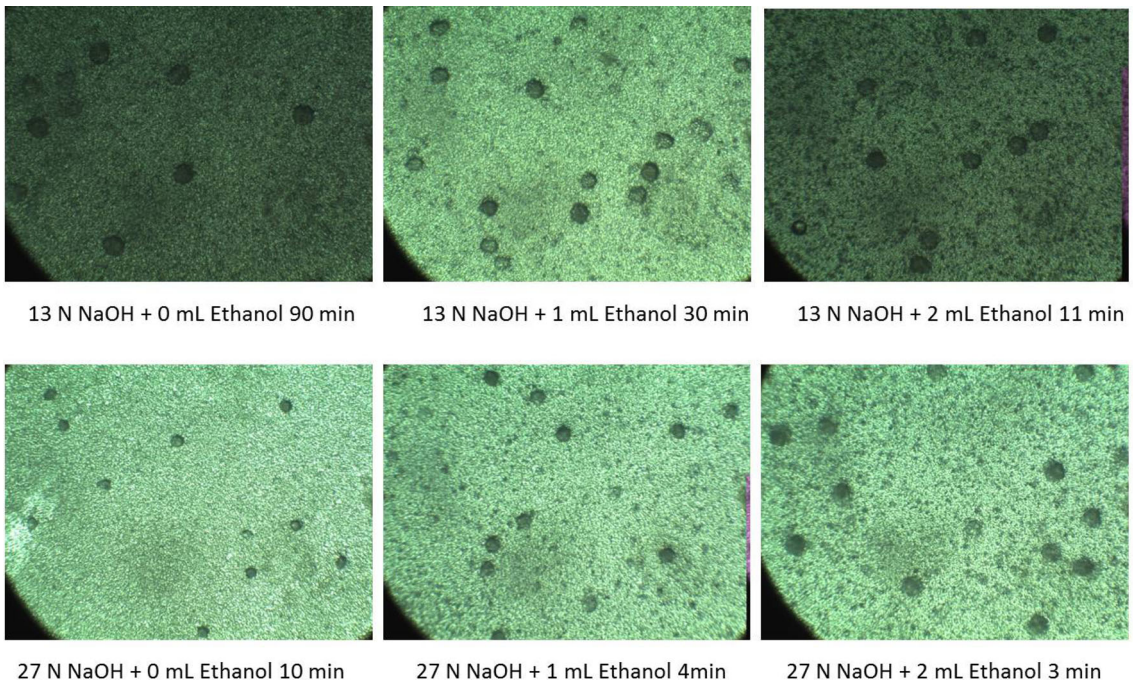

Fig. 6 (Color online) Selected optical micrographs of CR-39 detectors, etched under various etching conditions. Etching conditions are mentioned below each micrograph. Area of each micrograph is approximately 300 × 400 μm^2

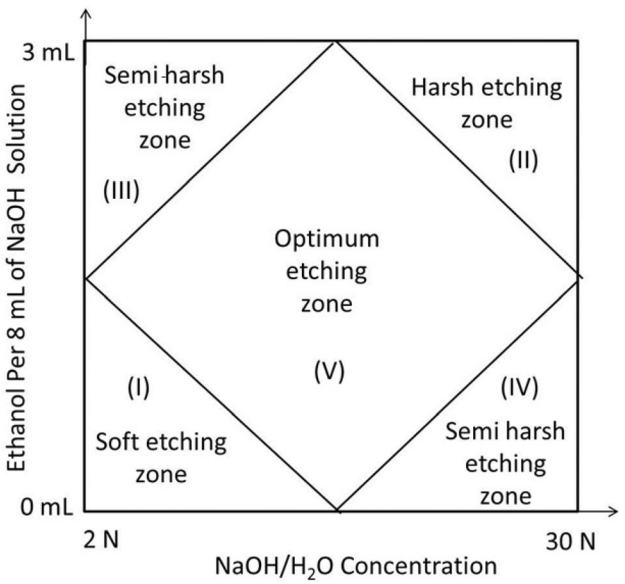

Fig. 7 Schematic plot showing NaOH/H_2O concentration and density of ethanol in the etching solution. The plot is divided into five etching zones

sense between proportional and exponential manners, and the Arrhenius equation no longer holds (semi-harsh and harsh etching zones). Regime III denotes concentrations greater than 25 N. In this regime, the bulk etch rate is saturated with respect to the etchant concentration. Limited diffusion of etching species in extremely dense etchant results in the saturation of the bulk etch of CR-39. We call this regime the diffusion-limited regime. The saturation of the bulk etch rate in Regime III of Fig. 3a and the decrease in reduced bulk etch rate in Regime II from Fig. 4 are new results. The major cause of this new and unexpected result, in our opinion, is the insulation of etching fronts caused by the deposition of etch products at extremely high etch rates and at highly viscous medium.

A comprehensive nuclear track chemical etching data bank is developed and presented in a unique manner and may prove quite useful for nuclear track researchers and students. A qualitative model is presented to explain the chemical bulk etching of the CR-39 detectors. The model differentiates between three characteristic regimes of bulk etching over an extensive range of etching conditions: 2 to 30 N NaOH/H_2O etching solution with ethanol (8 mL of NaOH/H_2O + 0 to 3 mL of ethanol). The role of ethanol in the etching of CR-39 polymer in NaOH/H_2O + ethanol etching solution should be further investigated microscopically and modeled quantitatively.

Acknowledgements The authors are deeply thankful to Dr. Yasser Rammah, Dr. Sameh Hassand and Eman Bebers for their valuable help and cooperation. The author Mushtaq Al-Jubbori is very grateful to the University of Mosul College of Education for Pure Science for their provided facilities, which helped to improve the quality of this work.

References

1. S.A. Gorbunov, R.A. Rymzhanov, N.I. Starkov et al., A model of chemical etching of olivine in the vicinity of the trajectory of a swift heavy ion. Nucl. Instr. Methods B **365**, 656 (2015). https://doi.org/10.1016/j.nimb.2015.09.074
2. M. Fromm, S. Kodaira, T. Kusumoto et al., Role of intermediate species in the formation of ion tracks in PADC: a review. Polym. Degrad. Stab. **161**, 213 (2019). https://doi.org/10.1016/j.polymdegradstab.2019.01.028
3. M.A. Al-Jubbori, Semi empirical equation for the calculation of the track diameter of alpha particles in CR-39 as a function of etching temperature. Raf. J. Sci. **25**, 120–126 (2014)
4. V.R. Oganesyan, V.V. Trofimov, S. Gaillard et al., Investigation of the response of thin CR-39 polymer foils irradiated with light ions. Nucl. Instr. Methods B **236**, 289 (2005). https://doi.org/10.1016/j.nimb.2005.03.257
5. T. Yamauchi, Studies on the nuclear tracks in CR-39 plastics. Radiat. Meas. **36**, 73 (2003). https://doi.org/10.1016/S1350-4487(03)00099-4
6. T. Kusumoto, Y. Mori, M. Kanasaki et al., Radiation chemical yields for the losses of typical functional groups in PADC films for high energy protons registered as unetchable tracks. Radiat. Meas. **87**, 35 (2016). https://doi.org/10.1016/j.radmeas.2016.01.029
7. M.A. Rana, Systematic measurements of etch induction time for nuclear tracks: Startup of etching and the multiplex effect. Nucl. Instr. Methods A **618**, 176 (2010). https://doi.org/10.1016/j.nima.2010.02.108
8. E.M. Awad, Multi-hit model on CR-39, DAM-ADC and LR-115 SSNTDs: statistical and comparative study. Radiat. Meas. **105**, 70 (2017). https://doi.org/10.1016/j.radmeas.2017.08.001
9. M.A. Rana, I.E. Qureshi, Studies of CR-39 etch rates. Nucl. Instr. Methods B **198**, 129 (2002). https://doi.org/10.1016/S0168-583X(02)01526-4
10. V. Ditlov, Formation model of bulk etching rate for polymer detectors. Radiat. Meas. **40**, 240 (2005). https://doi.org/10.1016/j.radmeas.2005.06.010
11. D. Hermsdorf, M. Hunger, S. Starke et al., Measurement of bulk etch rates for poly-allyl-diglycol carbonate (PADC) and cellulose nitrate in a broad range of concentration and temperature of NaOH etching solution. Radiat. Meas. **42**, 1 (2007). https://doi.org/10.1016/j.radmeas.2006.06.009
12. E.M. Awad, V.A. Ditlov, M. Fromm et al., Description of the bulk etching rate of CR-39 by an extended Arrhenius-like law in increased intervalls of temperature and etchant concentration. Radiat. Meas. **44**, 813 (2009). https://doi.org/10.1016/j.radmeas.2009.10.087
13. V.A. Ditlov, E.M. Awad, D. Hermsdorf et al., Interpretation of the bulk etching process in LR-115 detectors by the many-hit model. Radiat. Meas. **43**, S82 (2008). https://doi.org/10.1016/j.radmeas.2008.03.071
14. Y. Zhang, L. Liu, H. Wang et al., Primary yields of protons measured using CR-39 in laser-induced deuteron–deuteron fusion reactions. Nucl. Sci. Tech. **31**, 62 (2020). https://doi.org/10.1007/s41365-020-00769-8
15. B.G. Cartwright, E.K. Shirk, P.B. Price, A nuclear-track-recording polymer of unique sensitivity and resolution. Nucl. Instr. Methods **153**, 457 (1978). https://doi.org/10.1016/0029-554X(78)90989-8
16. Y. He, X. Xi, S. Guo et al., Calibration of CR-39 solid-state track detectors for study of laser-driven nuclear reactions. Nucl. Sci. Tech. **31**, 42 (2020). https://doi.org/10.1007/s41365-020-0749-1
17. S. Matiullah, W. Zaman. Rehman, Discovery of new etchants for CR-39 detector. Radiat. Meas. **39**, 337 (2005). https://doi.org/10.1016/j.radmeas.2004.06.012
18. Y. Zhang, H. Wang, Y. Ma et al., Energy calibration of a CR-39 nuclear-track detector irradiated by charged particles. Nucl. Sci. Tech. **30**, 87 (2019). https://doi.org/10.1007/s41365-019-0619-x
19. A.H. Ashry, A.M. Abdalla, Y.S. Rammah et al., The use of CH_3OH additive to NaOH for etching alpha particle tracks in a CR-39 plastic nuclear track detector. Radiat. Phys. Chem. **101**, 41 (2014). https://doi.org/10.1016/j.radphyschem.2014.03.037
20. M.A. Rana, CR-39 nuclear track detector: an experimental guide. Nucl. Instr. Methods A **910**, 121 (2018). https://doi.org/10.1016/j.nima.2018.08.077
21. E.M. Awad, Sameh Hassan, Eman Bebers et al., Bulk etch rate for PADC CR-39 at extended concentration range of NaOH mixed with ethanol and etchant viscosity study. Nucl. Instr. Methods B **464**, 45 (2020). https://doi.org/10.1016/j.nimb.2019.12.003
22. E.M. Awad, M.A. Rana, Bulk etch rates of CR-39 nuclear track detectors over a wide range of etchant (NaOH aqueous solution + ethanol) concentrations: measurements and modeling. Radiat. Eff. Defects Solids (2020). https://doi.org/10.1080/10420150.2020.1810038
23. Y.D. He, Can track-etch detector CR-39 record low-velocity GUT magnetic monopoles? Phys. Rev. D **57**, 3182 (1998). https://doi.org/10.1103/PhysRevD.57.3182
24. F. Kar, N. Asrslan, Effect of temperature and concentration on viscosity of orange peel pectin solutions and intrinsic viscosity–molecular weight relationship. Carbohyd. Polym. **40**, 277 (1999). https://doi.org/10.1016/S0144-8617(99)00062-4
25. H. Yanagie, K. Ogura, T. Matsumoto et al., Neutron capture autoradiographic determination of ^{10}B distributions and concentrations in biological samples for boron neutron capture therapy. Nucl. Instr. Methods A **424**, 122 (1999). https://doi.org/10.1016/S0168-9002(98)01284-4
26. E.M. Awad, S. Hassan, E. Bebers, Y.S. Rammah, Strong etching investigation on PADC CR-39 as a thick track membrane with deep depth profile study. Radiat. Phys. Chem. **177**, 109104 (2020). https://doi.org/10.1016/j.radphyschem.2020.109104
27. Y. Nishiura, S. Inoue, S. Kojima et al., Detection of alpha particles from ^{7}Li (p, α) ^{4}He and ^{19}F (p, α) ^{16}O reactions induced by laser-accelerated protons using CR-39 with potassium hydroxide–ethanol–water etching solution. Rev. Sci. Instr. **90**, 083307 (2019). https://doi.org/10.1063/1.5098863
28. R. Ogawara, T. Kusumoto, T. Konishi et al., Detection of alpha and ^{7}Li particles from $^{10}B(n, \alpha)^{7}Li$ reactions using a combination of CR-39 nuclear track detector and potassium hydroxide-ethanol-water solution in accelerator-based neutron fields. Nucl. Instr. Methods B **467**, 9 (2020). https://doi.org/10.1016/j.nimb.2020.01.030